

See discussions, stats, and author profiles for this publication at: <https://www.researchgate.net/publication/330843443>

Automated Scar Segmentation From Cardiac Magnetic Resonance-Late Gadolinium Enhancement Images Using a Deep-Learning Approach

Conference Paper · December 2018

DOI: 10.22489/CinC.2018.278

CITATIONS

0

READS

28

7 authors, including:



Sara Moccia

Università Politecnica delle Marche

21 PUBLICATIONS 30 CITATIONS

[SEE PROFILE](#)



Chiara Martini

University Hospital of Parma

114 PUBLICATIONS 1,008 CITATIONS

[SEE PROFILE](#)



Giuseppe Muscogiuri

Centro Cardiologico Monzino

74 PUBLICATIONS 331 CITATIONS

[SEE PROFILE](#)



Gianluca Pontone

Centro Cardiologico Monzino

379 PUBLICATIONS 3,393 CITATIONS

[SEE PROFILE](#)

Some of the authors of this publication are also working on these related projects:



NBI-Infframes dataset [View project](#)



The Laryngeal dataset [View project](#)

Automated Scar Segmentation From CMR-LGE Images Using a Deep Learning Approach

Sara Moccia^{1,2}, Riccardo Banali³, Chiara Martini⁴, Giuseppe Moscogiuri⁵, Gianluca Pontone⁵, Mauro Pepi⁵, Enrico Gianluca Caiani³

¹Department of Information Engineering, Università Politecnica delle Marche, Ancona, Italy

²Department of Advanced Robotics, Istituto Italiano di Tecnologia, Genoa, Italy

³Department of Electronics, Information and Bioengineering, Politecnico di Milano, Milan, Italy

⁴Diagnostic Department, Azienda Ospedaliera-Universitaria di Parma, Parma, Italy

⁵Clinical Cardiology Unit and Department of Cardiovascular Imaging, Centro Cardiologico Monzino IRCCS, Milan, Italy

Abstract

Aim. The presence of myocardial scar is a strong predictor of ventricular remodeling, cardiac dysfunction and mortality. Our aim was to assess quantitatively the presence of scar tissue from cardiac-magnetic-resonance (CMR) with late-Gadolinium-enhancement (LGE) images using a deep-learning (DL) approach. **Methods.** Scar segmentation was performed automatically with a DL approach based on ENet, a deep fully-convolutional neural network (FCNN). We investigated three different ENet configurations. The first configuration (C1) exploited ENet to retrieve directly scar segmentation from the CMR-LGE images. The second (C2) and third (C3) configurations performed scar segmentation in the myocardial region, which was previously obtained in a manual or automatic way with a state-of-the-art DL method, respectively. **Results.** When tested on 250 CMR-LGE images from 30 patients, the best-performing configuration (C2) achieved 97% median accuracy (inter-quartile (IQR) range = 4%) and 71% median Dice similarity coefficient (IQR = 32%). **Conclusions.** DL approaches using ENet are promising in automatically segmenting scars in CMR-LGE images, achieving higher performance when limiting the search area to the manually-defined myocardial region.

1. Introduction

The presence of nonviable scar tissue in the left ventricle (LV) allows assessing LV remodeling, as well as patient's cardiac dysfunction or mortality [1].

The presence of nonviable scar tissue is commonly

identified with cardiac magnetic resonance with late gadolinium enhancement (CMR-LGE) [2]. To perform CMR-LGE, Gadolinium (Gd) is injected intravenously. Gd deposits in the nonviable tissue resulting in hyperenhanced (HE) area in CMR-LGE images.

In clinical practice, the presence of scar tissue from CMR-LGE images is commonly assessed qualitatively using the AHA 17-segment model [3]. Nonetheless, several quantitative approaches have been proposed: a large class of methods exploit threshold-based or clustering techniques that require heavy operator intervention [4]. However, these approaches are barely able to tackle variability in images (e.g., noise, resolution and intensity level) and patients (e.g., scar location and extent).

Recently, deep learning (DL) methods based on convolutional neural networks (CNNs) have been proposed to tackle this variability. A CNN is made of convolutional layers, that extract image features through convolutional kernels, and fully-connected layers, that classify these features [5]. The convolutional kernels and the fully-connected layer weights are automatically learned during a training process.

CNN approaches for scar segmentation commonly extract features from image patches and assign a class (i.e., scar or background) to the patch central pixel. Nonetheless, advancements in DL in other fields are focusing on methodologies that directly provide image segmentation instead of pixel classification. These methodologies exploit fully-convolutional neural networks (FCNNs), where fully-connected layers are replaced by upsampling layers [5].

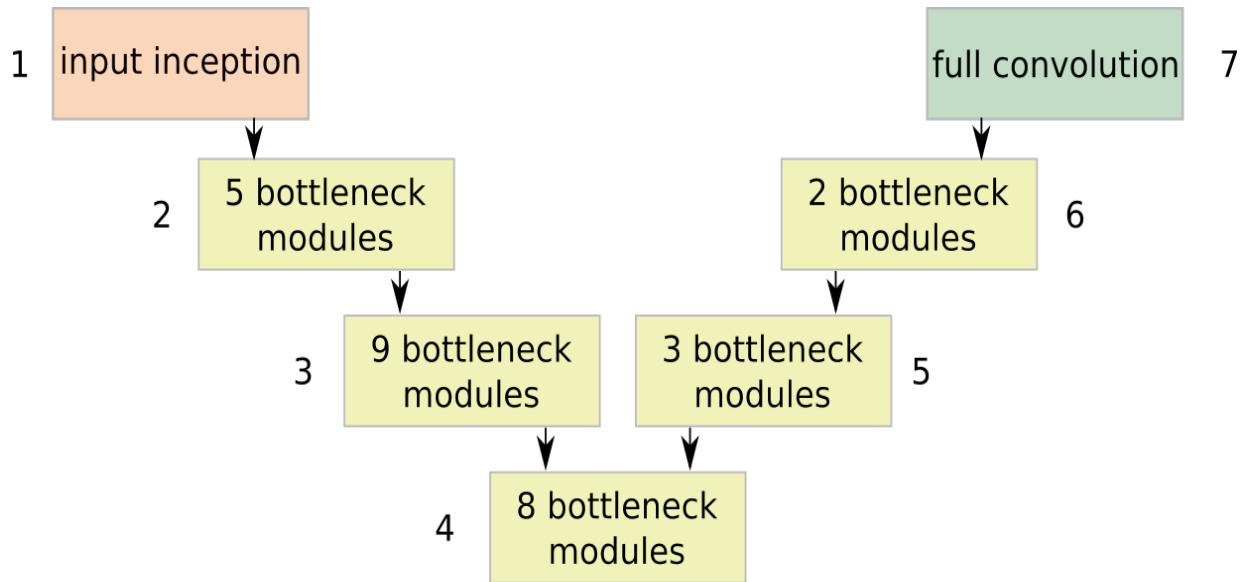


Fig. 1: ENet stages.

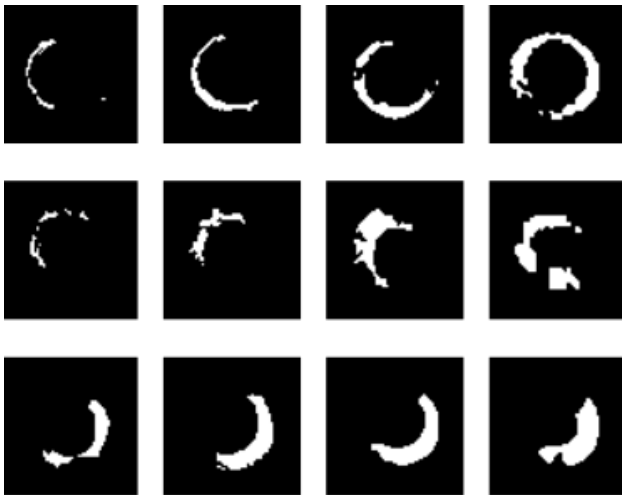


Fig. 2: Examples of scar masks obtained with manual tracing. Each row refers to a different patient. Masks are from apex (left) to base (right).

Inspired by these recent methodologies, the aim of this work was to assess quantitatively the presence of scar tissue in CMR-LGE images using a DL approach based on FCNNs.

2. Methods

In this work, a modified version of the efficient neural network (ENet) was exploited [6]. ENet was originally presented for natural-image segmentation and takes inspiration from residual networks. The architecture has 7 stages, as shown in Fig. 1.

The first stage was inspired to the inception module, and consisted of 13 convolutional kernels, with sizes

equal to 1x1, 3x3 and 5x5, in parallel with a 2x2 max-pooling layer.

Stages from 2 to 4 were made of bottleneck modules, as in [6], and acted as encoders for feature extraction. Stages from 5 to 6 acted as decoders and performed upsampling. In the decoder, max pooling and padding were replaced by max unpooling and spatial convolution without bias, respectively. The last stage was a bare full convolution with two channels (for the scar and background classes).

Spatial dropout, which improves the FCNN generalization ability by preventing activations from being strongly correlated, was also used.

2.1. Segmentation protocols

To perform scar segmentation, three different ENet configurations were considered. The first configuration (C1) exploited ENet to retrieve directly scar segmentation from the CMR-LGE images. The second (C2) and third (C3) configurations performed scar segmentation only in the myocardial region, previously obtained respectively in a manual or automatic way using a state-of-the-art DL method [7].

2.2. Training

For each segmentation protocol, training was performed with mini-batch gradient descent, using a batch size equal to 4. ADAM (with an initial learning rate equal to 5e-5) was used to optimize the cross entropy, which was chosen as loss function. The FCNNs was trained on 100 epochs. and the best model among epochs was chosen according to the Dice similarity coefficient (DSC):

$$DSC = 2 * TP / (FP + FN + 2 * TP) \quad (1)$$

where TP , FN are the number of scar pixels that are classified correctly and as background, respectively, and FP is the number of background pixels classified as scar tissue.

2.3. Evaluation

To test the three segmentation protocols, 250 short-axis CMR-LGE images of 30 patients (26 men and 4 women) with ischemic-heart disease were retrospectively selected and analyzed. Images were acquired at Centro Cardiologico Monzino in Milan, Italy using a 1.5-T scanner (Discovery MR450, GE Healthcare, Milwaukee, WI). Scar tissue was present in all patients, but only in 215 CMR-LGE images. Image size was 256x256 pixels (pixel resolution: 1.49x1.49 mm).

The ground-truth (GT) scar segmentation was manually obtained by an expert clinician using commercial software (Circle Cardiovascular Imaging v.5.6). LV-myocardial contours for protocol C2 were obtained in the same way. The datasets granted high intra- and inter-patient variability, as can be seen from Fig. 2 where sample scar masks are shown for three patients.

For each of the three protocols, CMR-LGE images were pre-processed prior to FCNN training and testing. In particular, CMR-LGE images were automatically cropped to reduce the processing area, as commonly suggested in the literature [8]. The circular structure was used to identify the LV cavity in the CMR-LGE image. Then, a squared cropping, centered on the LV center and with side equal to the 5/3 of the LV radius was performed. The crop operation was applied also to the corresponding GT masks. All the cropped images were resized to 64x64 and normalized for standardization. Finally, data augmentation was performed on the training set using 7 linear and non-linear transformations.

Considering the limited number of patients, leave-one-patient-out cross-validation was the method of choice to guarantee proper analysis. For each patient, the ENET trained on the remaining 29 patients was tested.

Segmentation performance was assessed with three

pixel-classification metrics: sensitivity (Se), specificity (Sp) and accuracy (Acc):

$$Se = (TP + FN) / TP \quad (2)$$

$$Sp = (TN + FP) / TN \quad (3)$$

$$Acc = (TP + TN) / (TP + TN + FP + FN) \quad (4)$$

where TN is the number of background pixels classified correctly. DSC was measured as overlap metric.

3. Results

With the best-performing configuration (C2), scar-segmentation median Acc and DSC were 97% (inter-quartile (IQR) range = 4%) and 71% (IQR = 32%), respectively. Sp and Se for C2 were 97% (IQR=3%) and 88% (IQR = 18%), respectively

C2 outperformed both C1 ($Acc = 96%$, $DSC = 55%$, $Sp = 97%$, $Se = 69%$) and C3 ($Acc = 95%$, $DSC = 51%$, $Sp = 97%$, $Se = 73%$), where Acc and DSC for automatic myocardial segmentation were 94% and 86%, respectively.

Visual segmentation examples are shown in Fig. 3.

4. Discussion

In this pilot study, as only 30 patients were included, data augmentation techniques allowed increasing the total number of available images up to 2000 and leave-one-patient-out cross-validation was the method of choice to guarantee proper analysis.

Computational training time was about 30 hours, and could be considered acceptable considering this approach and the use of not optimized computer architecture. The segmentation testing time was about 1s per CMR-LGE image.

All the three protocols showed a tendency to overestimate the scar contours with respect to the GT. This can be due to the fact that the FCNN recognized as part of the scar also those pixels belonging to moderate enhanced areas, possibly associated with hibernated tissue or border areas between scar and healthy tissue.

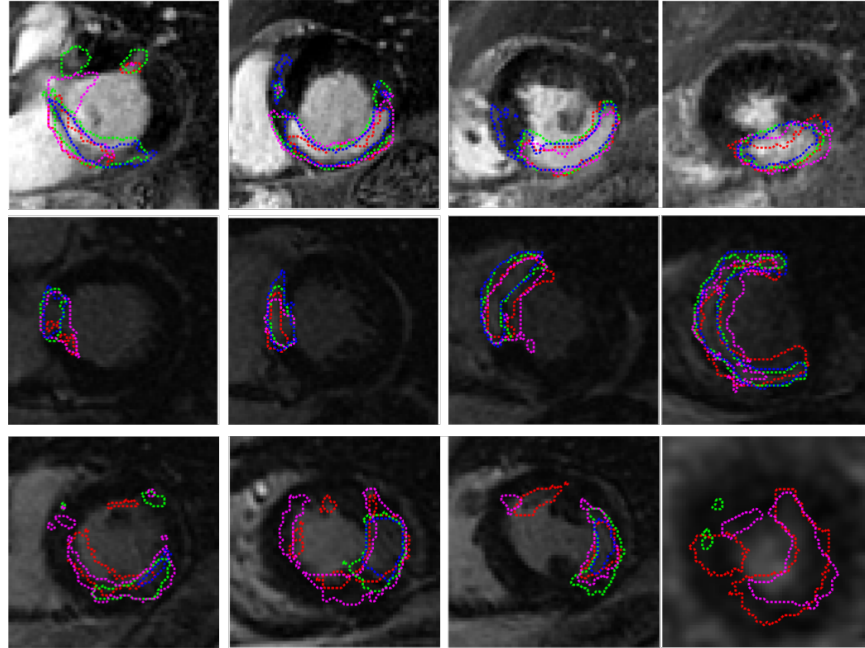


Fig. 3: Examples of segmentation obtained with C1 (red contour) , C2 (green contour) and C3 (magenta contour) for **three** patients. The blue contour refers to the manual tracing. Each row refers to a different patient.

5. Conclusion

ENet-based approaches are promising in automatically segmenting scar tissue in CMR-LGE images, achieving higher performance when limiting the search area to the manually-defined myocardial region. A complete automated approach still suffers from cumulative errors from both myocardial and scar segmentation.

Finally, it can be concluded that there are good margins for improvement in overcoming the limits that emerged during the development. By improving the quality of input images and consequently of GT masks, it will be possible to improve network learning. Furthermore, increasing the number of images and patients in the training dataset is likely to improve network performance.

References

- [1] Alexandre J, Saloux E, Dugue AE, Lebon A, Lemaitre A, Roule V, Labombarda F, Provost N, Gomes S, Scanu P, et al (2013) Scar extent evaluated by late gadolinium enhancement CMR: A powerful predictor of long term appropriate ICD therapy in patients with coronary artery disease. *Journal of Cardiovascular Magnetic Resonance* 15(1):12.
- [2] Kelle S, Roes SD, Klein C, Kokocinski T, de Roos A, Fleck E, Bax JJ, Nagel E (2009) Prognostic value of myocardial infarct size and contractile reserve using magnetic resonance imaging. *Journal of the American College of Cardiology* 54(19):1770-1777.
- [3] Mewton N, Revel D, Bonnefoy E, Ovize M, Croisille P (2011) Comparison of visual scoring and quantitative planimetry methods for estimation of global infarct size on delayed enhanced cardiac MRI and validation with myocardial enzymes. *European Journal of Radiology* 78(1):87-92.
- [4] Carminati MC, Boniotti C, Fusini L, Andreini D, Pontone G, Pepi M, Caiani EG (2016) Comparison of image processing techniques for nonviable tissue quantification in late gadolinium enhancement cardiac magnetic resonance images. *Journal of Thoracic Imaging* 31(3):168-176.
- [5] Moccia S, De Momi E, El Hadji S, Mattos LS (2018) Blood vessel segmentation algorithms: Review of methods, datasets and evaluation metrics. *Computer Methods and Programs in Biomedicine* 158:71-91.
- [6] Paszke A, Chaurasia A, Kim S, Culurciello E (2016) Enet: A deep neural network architecture for real-time semantic segmentation. *arXiv preprint arXiv:160602147*.
- [7] Lieman-Sifry J, Le M, Lau F, Sall S, Golden D (2017) Fastventricle: Cardiac segmentation with Enet. In: *International Conference on Functional Imaging and Modeling of the Heart*, Springer, pp 127-138.
- [8] Karim R, Bhagirath P, Claus P, Housden RJ, Chen Z, Karimghaloo Z, Sohn HM, Rodriguez LL, Vera S, Alba X, et al (2016) Evaluation of state-of-the-art segmentation algorithms for left ventricle infarct from late gadolinium enhancement MR images. *Medical Image Analysis* 30:95-107.

Address for correspondence:

Prof. Enrico G. Caiani

Dipartimento di Elettronica, Informazione e Bioingegneria

Politecnico di Milano

enrico.caiani@polimi.it